Femtosecond laser written plane-by-plane Bragg grating sensors in bioresorbable phosphate optical fibres

Antreas Theodosiou, *Member, IEEE*, Diego Pugliese, Edoardo Ceci-Ginistrelli, Nadia G. Boetti, Davide Janner, Daniel Milanese and Kyriacos Kalli, *Member, IEEE*

***Abstract*—We report on the realization of different types of optical sensors in a bioresorbable phosphate glass optical fibre using a femtosecond laser operating at 517 nm. We inscribed fibre Bragg grating-based optical filters such as uniform Bragg gratings, chirped gratings and Fabry-Perot cavities, using the plane-by-plane direct write inscription. The gratings were characterised in reflection and tested as sensors for temperature and relative humidity. We studied the stability and resilience of the gratings when inserted in high humidity environments (> 95%) for 52 h and observed the evolution of the grating characteristics during this period.**

***Index Terms*— Biosensors, fibre Bragg gratings, femtosecond laser, bioresorbable optical fibre.**

I. Introduction

OPTICAL and optoelectronic technologies have been widely used in biomedicine and healthcare related applications and the research efforts in these fields are dramatically expanding in several directions. A recent research direction arising from new advances in biomaterials science concerns the development of biomaterial-based photonic devices able to degrade in physiological conditions once their functionality has expired. To this aim, different materials capable of combining biodegradability with good optical properties have been synthesized.

The first biodegradable optical fibre was based on cellulose [1], whereas further studies led to the development of spider silk, fibroin and hydrogel-based devices [2-4]. Hydrogels, in particular, are gradually becoming the "gold standard" for bioresorbable optical devices given their evident resistance, flexibility and transparency [5].

Within this framework, calcium-phosphate glasses (CPGs) have been recently proposed as a promising alternative for the manufacture of resorbable devices [6]. These glasses, raising a strong interest as biomaterials since the 1980's, have been widely studied for the fabrication of bone scaffolds, resorbable composites and as support for neural growth [7-10]. CPGs offer superior optical properties in comparison to polymers, as they guarantee a wider window of transparency spanning from approximately 250 to 2600 nm. Moreover, their refractive index and dissolution kinetics can be tailored by conveniently changing the material composition.

CPG-based bioresorbable optical fibres have proven to be mechanically reliable both in dry and humid environments [11] and to show the lowest attenuation values in comparison to all resorbable photonic devices reported in the open literature. These fibres were recently employed for diffuse optics experiments on biological tissues showing the same performances as silica-based fibres [12], and their photosensitivity in deep ultraviolet (UV) region was also demonstrated [13].

In this work, we report on the application of femtosecond laser processing to the phosphate glass fibre to realise key optical components. We have used the direct-write, plane-by-plane (*Pl-by-Pl*) inscription method to inscribe bioresorbable optical grating sensors [14-17]. In particular, uniform fibre Bragg gratings (FBGs), chirped FBGs (CFBGs) and fibre Fabry-Perot (FFP) cavities were inscribed and characterised in reflection. In addition, the optical components were calibrated and used as temperature and relative humidity sensors. Finally, the FBG was tested in a high humidity environment over a 52 h period in a climate chamber.

Due to the high biocompatibility of the core and cladding calcium-phosphate glasses, the sensors developed in this work can be readily used as, for example, fibre optic breathing sensors to detect pressure inside the bloodstream or as local in-vivo temperature probes [18]. Indeed, given their bioresorbability, the same FBG and Fabry-Perot sensors normally used outside the body could be employed in-vivo and after their use be resorbed by the body itself. This could pave the way towards minimally invasive diagnostics and therapy

Antreas Theodosiou and Kyriacos Kalli are with the Photonics and Optical Sensors Research Laboratory, Cyprus University of Technology, Limassol 3036, Cyprus (e-mail: theodosiou.antreas@gmail.com, kyriacos.kalli@cut.ac.cy).

Diego Pugliese, Edoardo Ceci-Ginistrelli, and Davide Janner are with Dipartimento di Scienza Applicata e Tecnologia, Politecnico di Torino and RU INSTM, Corso Duca degli Abruzzi 24, 10129 Torino, Italy (e-mail: diego.pugliese@polito.it, edoardo.ceciginistrelli@polito.it, davide.janner@polito.it).

Daniel Milanese is with Dipartimento di Scienza Applicata e Tecnologia, Politecnico di Torino and RU INSTM, Corso Duca degli Abruzzi 24, 10129 Torino, Italy and Consiglio Nazionale delle Ricerche, Istituto di Fotonica e Nanotecnologie, Via alla Cascata 56/C, 38123 Trento, Italy (email: daniel.milanese@polito.it)

Nadia G. Boetti is with Fondazione LINKS – Leading Innovation & Knowledge for Society, Via P. C. Boggio 61, 10138 Torino, Italy (e-mail: boetti@ismb.it).

monitoring by using implanted optical fibres.

II. Materials And Methods

A. Fabrication and characterisation of the core and cladding glasses

The core and cladding glasses were synthesized by melting a powder batch of high purity (99+%) chemicals (P_2O_5, CaO, MgO, Na_2O, B_2O_3, SiO_2) within an alumina crucible at a temperature of 1200 °C for 1 h under a controlled atmosphere, followed by casting into preheated brass molds.

The core glass was cast into a cylindrical mold to form a rod, while two identical cladding tubes were shaped by rotational casting at a rotation speed of 3000 rpm using an equipment developed in-house. An additional cladding glass rod was fabricated only for characterization purposes.

Both the core and cladding components were annealed at a temperature close to the transition temperature (T_g) for 12 h to relieve the internal stresses and lastly were cooled slowly to room temperature. The obtained glasses were cut and optically polished to 1 mm-thick samples for optical and spectroscopic characterization. Other samples with thicknesses of 12 and 5 mm were employed for density and coefficient of thermal expansion (CTE) measurements, respectively, whereas 150 µm-thick cylindrical, single-material fibres were manufactured for dissolution tests in physiological conditions.

The density of the glasses was measured at room temperature by the Archimedes' method by using distilled water as immersion fluid with an estimated error of 0.005 g/cm^3.

The characterisation of the thermal properties (glass transition temperature T_g and onset crystallization temperature T_x) of the core and cladding glasses was carried out by differential thermal analysis (Netzsch DTA 404 PC Eos) up to 1200 °C with a heating rate of 5 °C/min in sealed Pt/Rh pans using ~ 200 mg of fine grain sample. The measurement also allowed for the assessment of the corresponding glass thermal stability and thus fibre ability, which can be considered proportional to the quantity $\Delta T = T_x - T_g$. An error of ± 3 °C was featured in measuring the characteristic temperatures.

The coefficient of thermal expansion (CTE) was measured with a horizontal alumina dilatometer (Netzsch DIL 402 PC) operating at 5 °C/min up to 1200 °C on 5 mm-long specimens. The measure was automatically interrupted when a shrinkage higher than 0.13% was reached (softening point). CTE values were calculated in the 200-400 °C temperature range featuring an error of ± 0.1 °C^{-1}.

The refractive index of the glasses was measured at 1533 nm by prism coupling technique (Metricon, model 2010). Ten scans were performed for each measurement, for which the estimated error of the measurement was ± 0.001.

The absorption spectra of the core and cladding glasses were measured at room temperature for wavelengths ranging from 190 to 800 nm using a double beam scanning spectrophotometer (Varian Cary 500) (Fig. 1). It is worth noting that the material loss at the operating wavelength of the femtosecond laser (517 nm), which is used to process the glass fibre, was < 0.1 dB/cm, thus making the material suitable for subsequent laser modification through multi-photon absorption, where the simultaneous absorption of low energy, high-density photons leads to material modification.

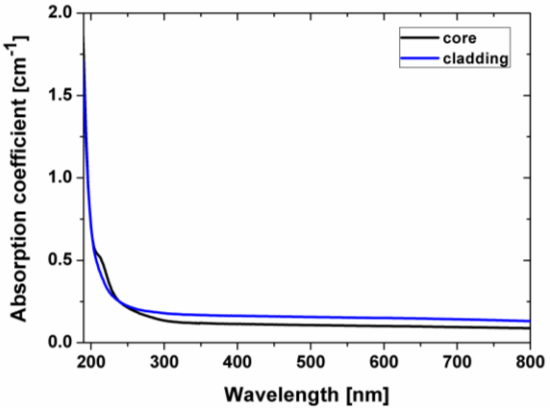

Fig. 1. Absorption spectra of the optical glasses used for fibre manufacturing as recorded from 190 and 800 nm.

Finally, the solubility of the glasses in physiological conditions was assessed performing a dissolution test on 1.5 cm-long sections of single material fibres. The test was performed in phosphate buffered saline solution (PBS, pH = 7.4, T = 37 °C) with a volume/exposed surface ratio of 0.1 ml/mm^2 and a refresh of the solution every three days. The fibres diameter and the pH of the solution were monitored following the procedure detailed in [6].

B. Fabrication and characterisation of the bioresorbable phosphate glass optical fibre

The bioresorbable phosphate glass optical fibre used for the grating inscriptions was manufactured by preform drawing, with the preform being obtained by the rod-in-tube technique [19]. The core glass rod was stretched to a 4-mm diameter cane and inserted into the first cladding tube. The fabricated core/cladding structure was then stretched to a 4-mm diameter rod and subsequently placed in the second cladding tube. The so-obtained final preform was finally heated above the T_g and below the T_x to draw the optical fibre. The fibre diameter was monitored during the drawing process.

All the stretching and drawing processes were carried out using a drawing tower developed in-house. The furnace consists of a graphite ring heated by induction operating at 248 kHz and delivering 170 W to reach the required drawing temperature (SAET, Torino, Italy).

Optical microscopy analysis was performed on different sections of the optical fibre to assess its dimensions and overall quality, whereas the attenuation losses of the fibre were measured by the cut-back technique using single-mode fibre pigtailed laser diode sources at 633 nm (QFLD-660-10S) and 1300 nm (Infineon SBM 52414x). Finally, the guiding ability of the optical fibre was investigated by taking a set of near-field images of the fibre cross-section at the wavelengths of 633 and 1300 nm using end-face coupled fibre pigtailed laser diode sources.

III. Results and Discussion

A. Physical, thermal, optical and spectroscopic properties of the core and cladding glasses

It has been demonstrated that the core and cladding calcium-phosphate glass compositions developed for this research could ensure an exclusive combination of optical and biological functionalities [6]. The fabricated glasses proved again to be homogeneous, stable against de-vitrification ($\Delta T \sim 200$ °C) and therefore suitable for crystal free fibre drawing; transparent from UV to near-infrared (NIR) region; soluble in simulated biological environment (PBS, pH = 7.4 at 37 °C) with a dissolution rate of around 4 μm/day. The optical and spectroscopic characterisation of the glasses was reported in detail in ref. [6]. Table 1 summarises the key thermal, physical, and optical properties of the manufactured core and cladding glasses.

Table 1. Glass transition temperature (T_g), onset crystallization temperature (T_x), glass stability parameter (ΔT), coefficient of thermal expansion (CTE), density and refractive index at 1533 nm of the manufactured calcium-phosphate core and cladding glasses.

Glass label	Core	Cladding
T_g [°C] ± 3 °C	435	435
T_x [°C] ± 3 °C	658	628
ΔT [°C] ± 6 °C	223	193
CTE [10^{-6} °C^{-1}] ± 0.1 °C^{-1}	12.6	12.2
ρ [g/cm^3] ± 0.005 g/cm^3	2.606	2.600
n ± 0.001	1.514	1.512

B. Characterisation of the bioresorbable phosphate glass optical fibre

The bioresorbable optical fibre showed diameters of 15 and 120 μm for the core and the cladding, respectively, with a corresponding numerical aperture (NA) value of 0.08. These parameters were designed to obtain single-mode (SM) behaviour at 1533 nm (V number = 2.390).

Moreover, a good interface adhesion between the core and cladding was observed, thus proving the noticeable thermo-mechanical compatibility of the two glasses (Fig. 2a). Furthermore, the near-field imaging of the fibre output recorded using an IR camera highlighted a good confinement of the light beam inside the core of the fibre (Fig. 2b).

Glass-based resorbable optical fibres show better light transmission properties if compared to their bio-compatible polymeric counterparts. In particular, the single-mode fibre used in this work is featured by attenuation loss coefficient values of 4.7 and 1.9 dB/m at 633 and 1300 nm, respectively, while similar loss is expected at 1550 nm. These values are in line with those typically exhibited by phosphate glass optical fibres [20], in comparison to loss values exceeding 20 dB/m for single-mode polymeric fibres [21].

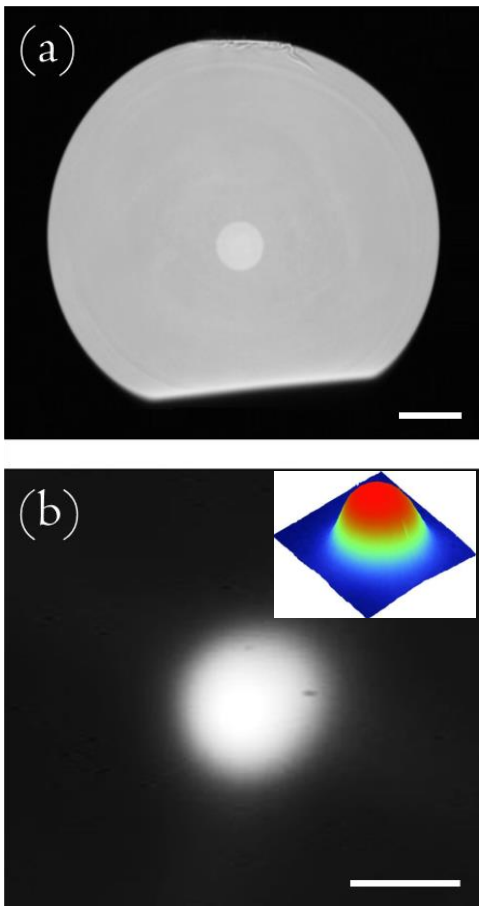

Fig. 2. a) Cross-section of the SM bioresorbable optical fibre; b) Near-field picture of the optical fibre showing the fundamental mode propagating at 1300 nm (inset: intensity normalized 3D beam profile). Scale bars equal to 20 μm.

IV. Inscription and Development of Optical Bio-Resorbable Sensors

In order to fully realise the potential of phosphate fibre for use in bio-sensing applications, it is important to be able to inscribe key optical components, such as Bragg gratings. This enables wavelength-encoded measurements to be made in-situ and in real time. Bragg gratings offer simple and well-known signal recovery, greatly simplifying the recovery of key information regarding the behaviour of the host material, in this case the phosphate fibre. To this extent, we have investigated the suitability of the phosphate fibre for femtosecond laser processing, focusing on direct-write laser inscription as this offers excellent flexibility in sensor development [22]. The goal was to inscribe and characterise uniform and chirped gratings and Fabry-Perot cavities. The inscription used a femtosecond laser (femtoRegen HighQ) operating at 517 nm with 220-fs pulse duration and a nanometre accuracy air-bearing translation stage system (Aerotech) for controlled and accurate two-axis motion during the inscription [23-25]. The fibre samples were carefully mounted on the translation stage and the laser beam was focused from above using a third stage, through a x50 microscope objective lens. The pulse energy at the exit of the laser was set to 100 nJ for a laser repetition rate of 2 kHz, controlled using a pulse picker.

For the inscription of the uniform fibre Bragg grating operating at 1563.08 nm, the grating period (Λ) was close to 2 μm (4th order FBG) and was selected to avoid any overlapping index change. The laser was swept perpendicularly to the fibre axis generating a plane across the fibre core and the inscription width was set at 15 μm (equal to the core diameter). The total number of periods was fixed to 1000, resulting in a ~ 2-mm grating length (L). The FBG transmission and reflection spectra (Fig.3a) were recovered using an optical spectrum analyser (OSA) with optical resolution of 10 pm through an optical circulator, with illumination from a broadband light-source (ASE730). From the spectra, the bandwidth full width at half maximum (FWHM) and the effective refractive index (n_{eff}) of the grating were found to be 0.5 nm and ~ 1.515, respectively, whereas the transmission notch of the FBG was ~1.5 dB, corresponding to a reflectivity of 30%. The effective index value coincides with the one measured during the glass manufacture (Table1). A microscope image of the femtosecond laser modification in the particular fibre core is shown in Fig.3b.

Subsequently, the inscription of a chirped grating was carried out. In this case the period of the grating was linearly increased with a chirp coefficient for each period as follows:

$$\Lambda_z = \Lambda_0 + k_z, \quad (1)$$

where Λ_0 is the initial period of the grating and k_z is the chirp coefficient for $0 < z < L$. The initial period was ~ 2.060 μm for the 4th order FBG at 1561 nm and the final period was ~ 2.067 μm, corresponding to a reflection wavelength of 1566 nm, and resulting in a 5-nm chirped grating, as shown in the reflection spectrum of Fig. 4. Ripples of up to 1 dB of the maximum reflection value were observed, however the ripples could potentially be reduced by using a smaller chirp coefficient and a higher number of periods.

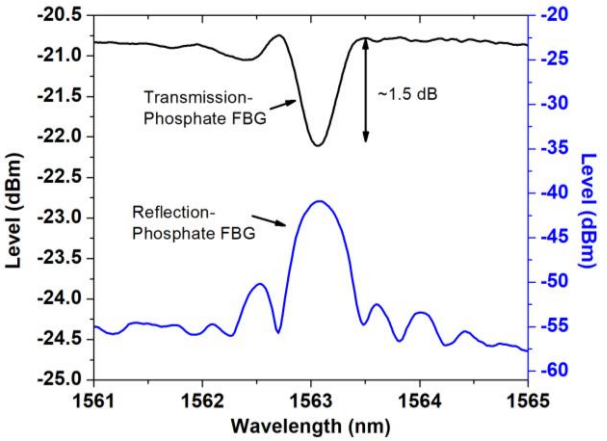

a)

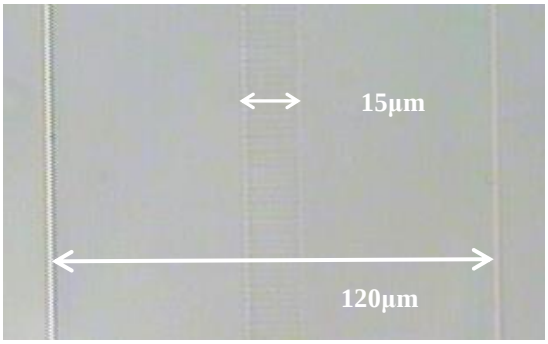

b)

Fig. 3. a) Reflection spectrum of a FBG inscribed in the phosphate fibre using the fs-laser, b) microscope picture of the laser-induced refractive index change.

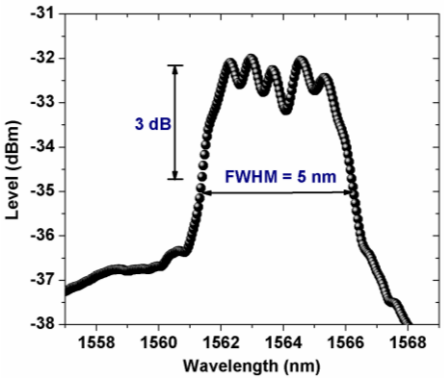

Fig. 4. Reflection spectrum of a 5-nm chirped grating inscribed in the bioresorbable phosphate fibre.

Finally, a FFP cavity was inscribed using two identical FBGs with a physical separation of 3.4 mm. The total cavity length must consider the light penetration depth through each grating and so is estimated to be the sum of the cavity length and approximately half of each grating length [26]. For gratings of length ~ 0.8 mm, the effective optical length of the cavity (L_{cavity}) is ~ 4.2 mm. The cavity free spectral range (FSR) is given by:

$$\lambda_{FSR} = \frac{\lambda^2}{2n_{eff}L_{cavity}}, \quad (2)$$

where λ is the wavelength of light and n_{eff} is the effective refractive index. According to the FBG inscription, n_{eff} was ~ 1.515 and for gratings operating at ~ 1561 nm the FSR is approximately equal to 190 pm. This is in full agreement with the experimental results shown in Fig. 5. The finesse of the fibre Fabry-Perot cavity is given by:

$$finesse = \frac{\lambda_{FSR}}{\delta\lambda} = \frac{4\sqrt{R_1R_2}}{\left(1-\sqrt{R_1R_2}\right)^2}, \quad (3)$$

where $\delta\lambda$ is the FWHM of the fringes and R_1 and R_2 are the maximum reflectivities of each grating. From (3), the calculated cavity finesse is 3.16, indicating an average grating reflectivity of ~ 53%. This result is anticipated given that each grating was made with less than 400 periods. The finesse and the reflectivity of the cavity could be improved by inscribing longer length Bragg gratings.

It is worth noting that the phosphate fibre employed in this

study is fragile and not production-ready. A diamond blade was used to cleave the fibre manually, consistently offering a high success rate, and cleave angles <10° were obtained. The phosphate fibre was fusion spliced with a standard SMF28 pigtail using modified splice settings on a Fujikura FSM 100P+ fusion splicer.

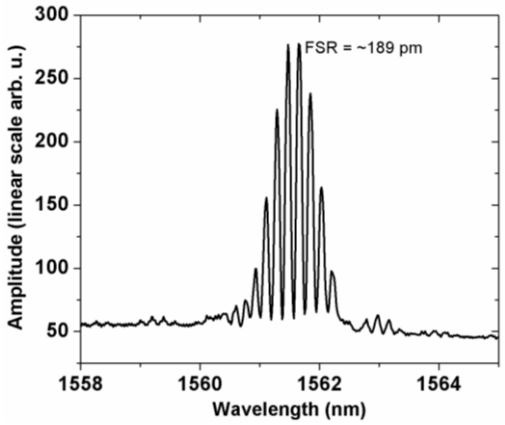

Fig. 5. Reflection spectrum of a Fabry-Perot cavity inscribed in the bioresorbable phosphate fibre using two identical FBGs, recovered using a commercial grating demodulator.

V. Characterisation and Calibration of the Bioresorbable Optical Sensors

The bioresorbable sensors so realized could be embedded in different parts of the human's body to precisely measure pressure, temperature, acidity or other parameters of interest in biomedicine and clinical care. To this aim, it is essential to study the behaviour of the sensors when inserted in environments with high water content, such as human blood. In addition, the sensor response to temperature changes is fundamental, since cross sensitivity issues could cause measurement inaccuracies. Therefore, the uniform bioresorbable phosphate FBG was placed in a climate chamber (Memmet 108HCP) and interrogated in reflection. The characterisation measurements began with the temperature sensitivity. The relative humidity (RH) of the chamber was kept constant at 35%, whereas the temperature was set to increase from 23 to 73 °C in a one-hour cycle. During this period, snapshots of the reflection spectrum were captured, and the temperature detected by the climate chamber sensor was recorded. The temperature response of the grating was found to be 12.7 pm/°C, as shown in Fig. 6, and compares to the 10.5 pm/°C typically measured for standard single-mode optical glass fibres. Moreover, a noticeable increase of the FBG peak amplitude was observed as the temperature was increased from 25.3 to 73.1 °C (Fig. 7). The amplitude increase of the FBG with temperature could be related to changes in coupling at the splice joint, and the disparity in NA between the two fibres.

For the humidity tests the climate chamber temperature was kept constant (36 °C) and the RH was increased from 35 to 95%. After 4 h, the FBG wavelength shifted by only 0.025 nm, as shown in Fig. 8, thus leading to a low response to RH of 0.416 pm/% RH. The grating was kept under these conditions for 52 h and its reflection spectrum was recorded every 6 h. Over the 52 h, the grating profile, amplitude and reflection wavelength noticeably changed, with a significant decrease of the grating amplitude and its complete disappearance at 52 h. The reflection spectra of the grating in the climate chamber for different time intervals up to 52 h are shown in Fig. 9, whereas Fig. 10 shows the change in grating amplitude *vs.* time in the chamber. This amplitude drop can be correlated with the property of the phosphate fibre to dissolve during water absorption. The response is analogous to that exhibited by a recently reported tilted-FBG inscribed in a similar phosphate glass fibre with an excimer laser operating at 193 nm [27].

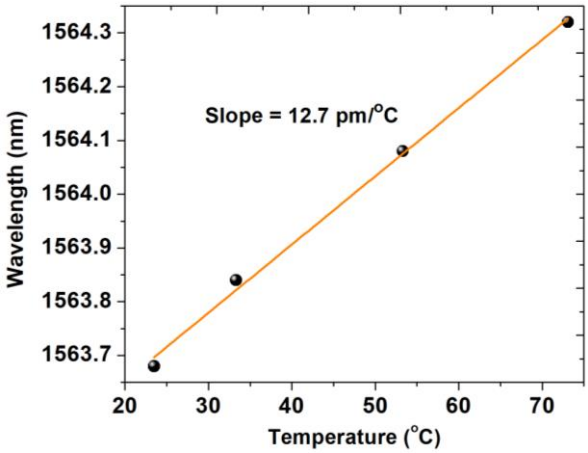

Fig. 6. Temperature response of the uniform FBG inscribed in the bioresorbable phosphate fibre using the *Pl-by-Pl* femtosecond laser inscription method.

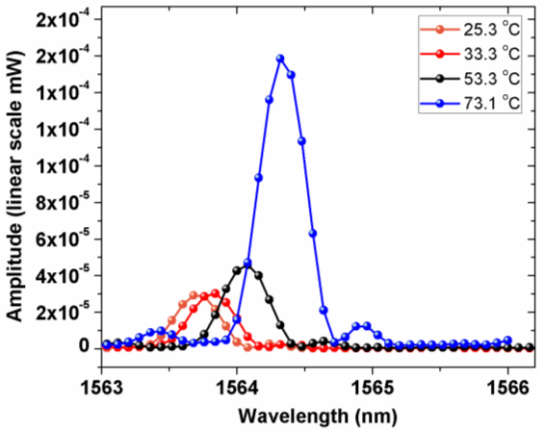

Fig. 7. Amplitude change of the uniform FBG inscribed in the bioresorbable phosphate fibre as the temperature increases.

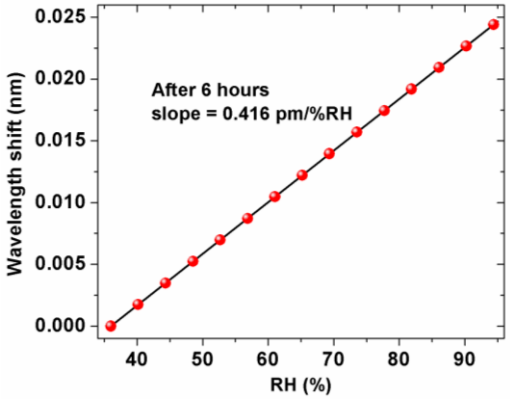

Fig. 8. Response of the uniform FBG when the environmental RH was increased from 35 to 90% at a constant temperature (~ 36 °C).

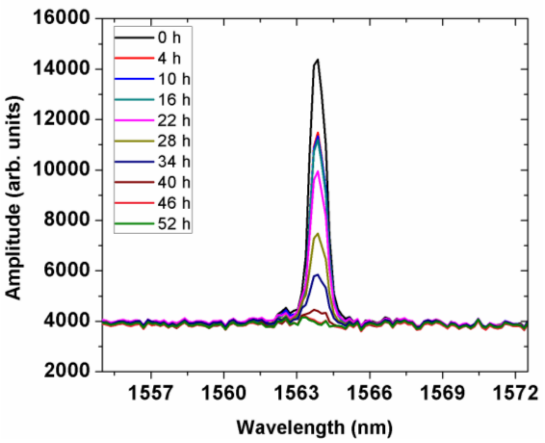

Fig. 9. Reflection spectra of the uniform FBG inscribed in the bioresorbable phosphate fibre when inserted in a climate chamber with 95% RH for different time intervals.

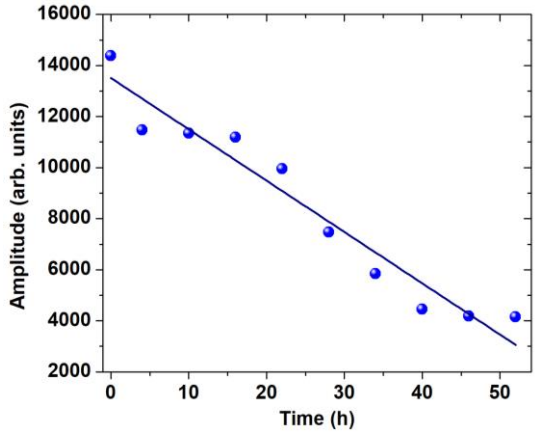

Fig. 10. Amplitude modulation of the phosphate FBG when inserted in a climate chamber with high RH levels. The filled circles represent the experimental data, while the continuous line is the linear fitting curve.

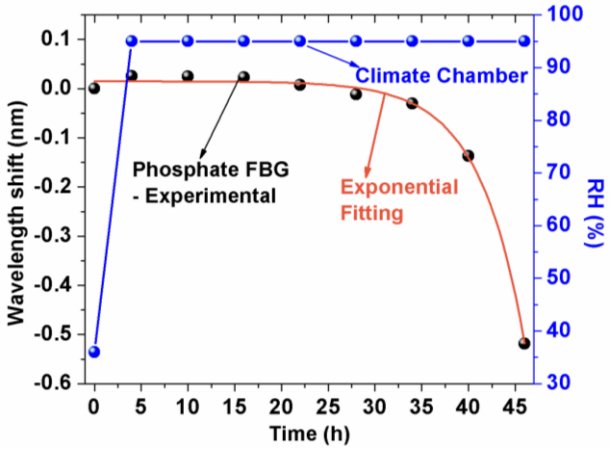

Fig. 11. Wavelength shift of the phosphate Bragg grating when inserted in a climate chamber with 95% RH for different time intervals.

In order to assess the grating response in high RH environments the climate chamber was kept at 95% RH over the 52 h and the Bragg wavelength shift was assessed using the ZCA to improve the resolution of our results (< 1 pm) [28]. The outcomes of this measurement are shown in Fig. 11, where the blue line represents the RH level inside the climate chamber as detected by the chamber sensor, and the red line depicts the response of the FBG. The Bragg wavelength shift at 52 h was not reported, since the FBG magnitude was very close to the noise floor and hence it was not possible to demodulate the weak signal. The Bragg wavelength exhibited an initial red-shift up to the first 4 h as previously shown in Fig. 8 and a subsequent blue-shift following an exponential decay rate. The former indicates water absorption in the first 4 h, leading to a change in the fibre dimensions. As a result, an increase of the grating period and an accompanying positive shift in the resonance wavelength occurred. This absorption, after several hours, appeared to selectively etch the laser-exposed refractive index modulated zones of the FBG in the centre of the core, since there was no clear indication of cladding diameter decreasing under the microscope. This opinion is supported by the observed negative wavelength shift associated with a drop in the effective refractive index of the FBG. To support our conviction, we inscribe a weaker grating maintaining the inscription parameters (number of periods, repetition rate, grating length) as before, but with a reduction in the pulse energy to 68 nJ. The induced index change is subsequently reduced, and there is a relative blue shift of ~140 pm for the weaker FBG (Fig. 12). We believe that the 'strong' FBG weakens with humidity, because of partial erasure, and indeed is observed to blue shift in wavelength as the humidity increases, supporting this hypothesis. The wavelength difference between the two FBGs is equivalent to the wavelength shift experienced by the FBG in the climate chamber after ~35 hours, according to Fig. 11. This is under further investigation.

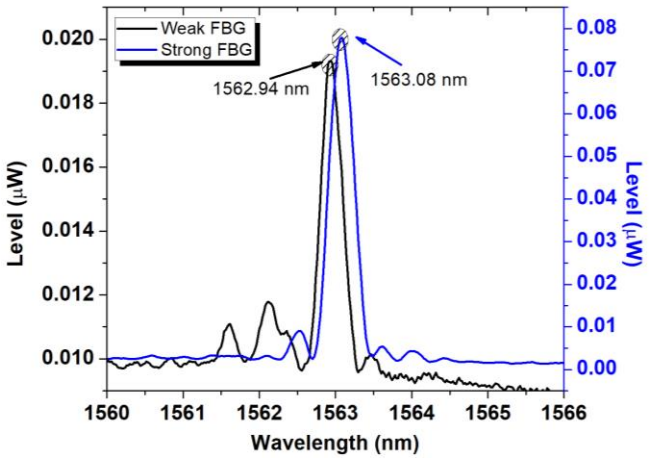

Fig. 12. Reflection spectra of relatively weak and strong phosphate fibre FBGs, with a wavelength difference of 140 pm.

VI. Conclusion

We report on the first fabrication (to the authors' knowledge) of femtosecond laser optical devices in a bioresorbable phosphate glass optical fibre. Uniform and chirped fibre Bragg gratings and a fibre Fabry-Perot cavity were inscribed using the direct-write *Pl-by-Pl* technique. The uniform grating was initially characterised for changes to relative humidity and temperature and showed sensitivities of 0.416 pm/% RH and 12.7 pm/°C, respectively. The RH sensitivity, assessed after the grating had been maintained for 4 h inside a climate chamber

with 95% RH, proved to be very low, as expected when dealing with a glass-based fibre. The temperature sensitivity was similar to that exhibited by glass fibres [29].

Subsequently, the grating sample was kept for up to 52 h into the climate chamber at 95% RH; the grating showed a significant profile distortion and its amplitude progressively decreased, whereas the resonance wavelength of the grating shifted towards shorter wavelengths, indicating erasure.

We consider that this work is extremely important for the development and characterisation of biocompatible and bioresorbable optical sensors and represents a significant step forward, enabling potential applications in the biomedical domain for both diagnosis and treatment.

ACKNOWLEDGMENT

The authors acknowledge the COST Action MP1401 "Advanced Fibre Laser and Coherent Source as tools for Society, Manufacturing and Lifescience" for the support of this research effort. The authors also acknowledge the Interdepartmental Center PhotoNext of Politecnico di Torino for supporting the activity of optical fibre fabrication. D.J. acknowledge support from Compagnia di San Paolo through the Starting Grant program.

REFERENCES

[1] A. Dupuis, N. Guo, Y. Gao, N. Godbout, S. Lacroix, C. Dubois, and M. Skorobogatiy, "Prospective for biodegradable microstructured optical fibers," *Opt. Lett.*, vol. 32, no. 2, pp. 109–111, Jan. 2007.

[2] S. Kujala, A. Mannila, L. Karvonen, K. Kieu, and Z. Sun, "Natural silk as a photonics component: a study on its light guiding and nonlinear optical properties," *Sci. Rep.*, vol. 6, Art. no. 22358, Mar. 2016.

[3] A. K. Yetisen, *H. Butt, L. R. Volpatti, I. Pavlichenko, M. Humar, S. J. Kwok, H. Koo, K. S. Kim, I. Naydenova,* A. Khademhosseini, S. K. Hahn, and S. H. Yun, "Photonic hydrogel sensors," *Biotechnol. Adv.*, vol. 34, no. 3, pp. 250–271, May-Jun. 2016.

[4] M. Choi, J. W. Choi, S. Kim, S. Nizamoglu, S. K. Hahn, and S. H. Yun, "Light-guiding hydrogels for cell-based sensing and optogenetic synthesis *in vivo*," *Nat. Photonics*, vol. 7, pp. 987–994, Dec. 2013.

[5] S. Nizamoglu, *M. C. Gather, M. Humar, M. Choi, S. Kim, K. S. Kim, S. K. Hahn, G. Scarcelli, M. Randolph, R. W. Redmond, and S. H. Yun*, "Bioabsorbable polymer optical waveguides for deep-tissue photomedicine," *Nat. Commun.*, vol. 7, Art. no. 10374, Jan. 2016.

[6] E. Ceci-Ginistrelli, D. Pugliese, N. G. Boetti, G. Novajra, A. Ambrosone, J. Lousteau, C. Vitale-Brovarone, S. Abrate, and D. Milanese, "Novel biocompatible and resorbable UV-transparent phosphate glass based optical fiber," *Opt. Mater. Express*, vol. 6, no. 6, pp. 2040–2051, Jun. 2016.

[7] J. Burnie, T. Gilchrist, S. R. I. Duff, C. F. Drake, N. G. L. Harding, and A. J. Malcolm, "Controlled release glasses (C.R.G.) for biomedical uses," *Biomaterials*, vol. 2, no. 4, pp. 244–246, Oct. 1981.

[8] A. S. Monem, H. A. ElBatal, E. M. Khalil, M. A. Azooz, and Y. M. Hamdy, "In vivo behavior of bioactive phosphate glass-ceramics from the system P_2O_5-Na_2O-CaO containing TiO_2," *J. Mater. Sci. Mater. Med.*, vol. 19, no. 3, pp. 1097–1108, Mar. 2008.

[9] N. J. Lakhkar, I. -H. Lee, H. -W. Kim, V. Salih, I. B. Wall, and J. C. Knowles, "Bone formation controlled by biologically relevant inorganic ions: role and controlled delivery from phosphate-based glasses," *Adv. Drug Delivery Rev.*, vol. 65, no. 4, pp. 405–420, Apr. 2013.

[10] G. Novajra, *et al*., "Bioactive glasses for nerve regeneration," in *Bioactive glasses: fundamentals, technology and applications*, A. R. Boccaccini, D. S. Brauer and L. Hupa, Eds., Cambridge: RSC, 2017, pp. 420–441.

[11] V. M. Sglavo, D. Pugliese, F. Sartori, N. G. Boetti, E. Ceci-Ginistrelli, G. Franco, and D. Milanese, , "Mechanical properties of resorbable calcium-phosphate glass optical fiber and capillaries," *J. Alloys Compd.*, vol. 778, pp. 410–417, Mar. 2019.

[12] L. Di Sieno, *et al.*, "Towards the use of bioresorbable fibers in time-domain diffuse optics," *J. Biophotonics*, vol. 11, no. 1, Art. no. e201600275, Jan. 2018.

[13] M. Konstantaki, S. Pissadakis, D. Pugliese, E. Ceci-Ginistrelli, N. G. Boetti and D. Milanese, "Bragg grating UV inscription in a bioresorbable phosphate glass optical fiber," in *18th International Conference on Transparent Optical Networks (ICTON)*, Trento, Italy, 2016, pp. 1-4.

[14] A. Theodosiou, A. Lacraz, A. Stassis, C. Koutsides, M. Komodromos, and K. Kalli, "Plane-by-plane femtosecond laser inscription method for single-peak Bragg gratings in multimode CYTOP polymer optical fiber", *J. Lightwave Technol.*, vol. 35, no. 24, pp.5404–5410, Dec. 2017.

[15] A. Ioannou, A. Theodosiou, C. Caucheteur, and K. Kalli, "Direct writing of plane-by-plane tilted fiber Bragg gratings using a femtosecond laser", *Opt. Lett.*, vol. 42, no. 24, pp. 5198–5201, Dec. 2017.

[16] K. Kalli, A. Theodosiou, A. Ioannou and A. Lacraz, "Femtosecond laser processing of optical fibres for novel sensor development", in *25th Optical Fiber Sensors (OFS) Conference*, Jeju, Korea, 2017, pp. 1–4.

[17] A. Theodosiou, A. Lacraz, M. Polis, K. Kalli, M. Tsangari, A. Stassis, and M. Komodromos, "Modified fs-laser inscribed FBG array for rapid mode shape capture of free-free vibrating beams", *IEEE Photonics Technology Technol. Lett.*, vol. 28, no. 14, pp. 1509–1512, Jul. 2016.

[18] F. C. Favero, *V. Pruneri, J. Villtoro*, "Microstructured optical fiber interferometric breathing sensor", *J. of Biomedical Optics*, vol. 17, no 3, 037006, 2012

[19] N. G. Boetti, G. C. Scarpignato, J. Lousteau, D. Pugliese, L. Bastard, J. -E. Broquin, and D. Milanese, "High concentration Yb-Er co-doped phosphate glass for optical fiber amplification," *J. Opt.*, vol. 17, Art. no. 065705, Jun. 2015.

[20] Y. W. Lee, S. Sinha, M. J. F. Digonnet, R. L. Byer, and S. Jiang, "20 W single-mode Yb^{3+}-doped phosphate fiber laser," *Opt. Lett.*, vol. 31, no. 22, pp. 3255–3257, Nov. 2006.

[21] J. Guo, *et al*., "Highly stretchable, strain sensing hydrogel optical fibers," *Adv. Mater.*, vol. 28, no. 46, pp. 10244–10249, Dec. 2016.

[22] G. N. Smith, K. Kalli, and K. Sugden "Advances in femtosecond machining and inscription of micro and nano photonic devices" in *Frontiers in guided wave optics and optoelectronics*, B. Pal, Ed., London: IntechOpen, 2010, pp. 295–320.

[23] M. Fokine, A. Theodosiou, S. Song, T. Hawkins, J. Ballato, K. Kalli, and U. J. Gibson, "Laser structuring, stress modification and Bragg grating inscription in silicon-core glass fibers", *Opt. Mater. Express*, vol. 7, no. 5, pp. 1589–1597, May 2017.

[24] A. Theodosiou, X. Hu, C. Caucheteur, and K. Kalli, "Bragg gratings and Fabry-Perot cavities in low-loss multimode CYTOP polymer fiber", *IEEE Photonics Technol. Lett.*, vol. 9, no. 30, pp. 857–860, May 2018.

[25] A. Theodosiou, *A. Ioannou, M. Polis, A. Lacraz, C. Koutsides and K. Kalli*, "Femtosecond laser waveguide and FBG inscription in four-core optical fibre", in *SPIE Photonics Europe 2016*, Brussels, Belgium, 2016, Art. no. 99860F.

[26] Y. O. Barmenkov, *et al.*, "Effective length of short Fabry-Perot cavity formed by uniform fiber Bragg gratings", *Opt. Express*, vol. 14, no. 14, pp. 6394–6399, Jul. 2006.

[27] D. Pugliese, *et. al.*, "Bioresorbable optical fiber Bragg gratings", *Opt. Lett.*, vol. 43, no. 4, pp. 671–674, Feb. 2018.

[28] A. Theodosiou, M. Komodromos, and K. Kalli, "Accurate and fast demodulation algorithm for multipeak FBG reflection spectra using a combination of cross correlation and Hilbert transformation", *J. Lightwave Technol.*, vol. 35, no. 18, pp. 3956–3962, Sept. 2017.

[29] A. Othonos and K. Kalli, *Fiber Bragg gratings: fundamentals and applications in telecommunications and sensing*. Boston, MA, USA: Artech House Optoelectronics Library, 1999.